Decision Analytics Journal 10 (2024) 100420

Contents lists available at ScienceDirect

Decision Analytics Journal

journal homepage: www.elsevier.com/locate/dajour

An empirical wavelet transform-based approach for motion artifact removal in electroencephalogram signals

Abhay B. Nayak [a], Aastha Shah [a], Shishir Maheshwari [b,*], Vijay Anand [c], Subrata Chakraborty [d], T. Sunil Kumar [e]

[a] Department of Electronics and Instrumentation, Birla Institute of Technology & Science, Pilani, Rajasthan, 333031, India
[b] Department of Electronics & Communication Engineering, Thapar Institute of Engineering & Technology, Patiala, Punjab, India
[c] Wipro Ltd., India
[d] School of Science & Technology, University of New England, Armidale, Australia
[e] Department of Electrical Engineering, University of Gävle, Sweden

ARTICLE INFO

Keywords:
Empirical wavelet transform (EWT)
Motion artifact
Intrinsic mode function (IMF)
Electroencephalogram (EEG)
Principal component analysis
Noise removal

ABSTRACT

Motion artifacts reduce the quality of information in the electroencephalogram (EEG) signals. In this study, we have developed an effective approach to mitigate the motion artifacts in EEG signals by using empirical wavelet transform (EWT) technique. Firstly, we decompose EEG signals into narrowband signals called intrinsic mode functions (IMFs). These IMFs are further processed to suppress the artifacts. In our first approach, principal component analysis (PCA) is employed to suppress the noise from these decomposed IMFs. In the second approach, the IMFs with noisy components are identified using the variance measure, which are then removed to obtain the artifact-suppressed EEG signal. Our experiments are conducted on a publicly available Physionet dataset of EEG signals to demonstrate the effectiveness of our approach in suppressing motion artifacts. More importantly, the IMF-variance-based approach has provided significantly better performance than the EWT-PCA based approach. Also, the IMF-variance based approach is computationally more efficient than the EWT-PCA based approach. Our proposed IMF-variance based approach achieved an average signal to noise ratio (ΔSNR) of 28.26 dB and surpassed the existing methods developed for motion artifact removal.

1. Introduction

Electroencephalogram (EEG) quantitatively measures the human brain's electrical activity which takes place due to the firing of neurons [1] and such brain activity is recorded non-invasively utilizing several electrodes located in different regions of the scalp [2]. EEG is widely used to detect Alzheimer's disease [3,4], schizophrenia [5,6], sleep disorders [7,8], strokes [9], anaesthesia depth [10] and cognitive impairment [11,12]. EEG can also be used to detect epileptic seizures [13–16], human emotions [17–19], estimate drowsiness levels [20,21] and develop brain–computer interfaces (BCIs) [22–24].

EEG is a vital biological indicator; however, it is quite prone to motion artifacts caused by the voluntary or the involuntary movement of the patient while recording the EEG data. The measuring instruments are extremely sensitive and are susceptible to even movements as subtle as the blinking of eyes [25]. Additionally, to obtain high-quality EEG data we require the impedance of the electrodes in contact with the skin to be sufficiently low [26]. This is why traditionally data recording has required the use of conductive gel and proper skin preparation, but this approach is valid only for small durations since the gel dries out after a couple of hours [26]. Recent advances have introduced dry electrodes but the quality of the signal recorded is degraded [27,28]. Motion artifacts are the most devastating disturbances faced with dry electrodes and is the most important challenge yet to be addressed for the purpose of robust long term EEG monitoring [26].

These artifacts can hinder the performance of EEG-based systems [25]. Primarily, there are 2 types of signal corrupting artifacts — physiological and the non-physiological. The physiological artifacts are introduced by the routine electrical activity of the body. These include those generated by the eyes, tongue, heart, muscles, and even sweat glands [25]. The non-physiological artifacts are generated by the electromagnetic fields outside the body. Some examples of non-physiological artifacts are those introduced by the medical or data sampling instruments, 60 Hz artifact, electrode artifact [25]. Therefore, it is important to suppress these artifacts. In this paper, we primarily focus on removing motion artifacts in EEG signals using the empirical wavelet transform (EWT) technique.

* Corresponding author.
E-mail addresses: nenabhay@gmail.com (A.B. Nayak), aasthashah1904@gmail.com (A. Shah), shishir.maheshwari@thapar.edu (S. Maheshwari), vijayanand.phd20@gmail.com (V. Anand), Subrata.Chakraborty@uts.edu.au (S. Chakraborty), sunilkumar.telagam.setti@hig.se (T.S. Kumar).

https://doi.org/10.1016/j.dajour.2024.100420
Received 11 July 2023; Received in revised form 30 January 2024; Accepted 8 February 2024
Available online 10 February 2024

Various methodologies have been explored in previous attempts to mitigate motion artifacts and eliminate noise from corrupted EEG signals. One such approach involves singular spectrum analysis (SSA) [29], which has been proposed for EEG denoising. In this method, SSA [30] is applied to decompose the single-channel EEG data, followed by the removal of motion-corrupted segments using adaptive noise cancellation (ANC).

Approaches outlined in [31–33] employ either empirical mode decomposition (EMD) or ensemble empirical mode decomposition (EEMD). EMD breaks down a signal into a finite and often small number of 'intrinsic mode functions' that allow well-behaved Hilbert transforms [32]. Approaches in [31–33] operate under the assumption that motion artifact information is present in either one or multiple sub-band signals. These sub-band signals are derived by decomposing the motion-corrupted EEG signal using time–frequency techniques. The decomposed sub-bands undergo processing to eliminate noise. Subsequently, these processed sub-band signals are combined to reconstruct a noise-suppressed EEG signal.

Sweeney et al. [31] employed various single-stage and two-stage techniques for removing motion artifacts, utilizing the discrete wavelet transform (DWT). DWT is a transformation that breaks down a given signal into several sets, where each set represents a time series of coefficients describing the signal's time evolution in the corresponding frequency band [34,35]. Additionally, Sweeney et al. explored approaches such as empirical mode decomposition (EMD) cascaded with canonical correlation analysis (EMD-CCA) and ensemble empirical mode decomposition (EEMD) coupled with canonical correlation analysis (EEMD-CCA) [31]. These techniques involve the decomposition of single-channel EEG signals and use the autocorrelation function, along with a motion artifact-free reference signal, to identify and discard the corrupted components [36].

In another study [32], EMD, coupled with independent component analysis (ICA) referred to as EMD-ICA, was utilized. Independent component analysis is a statistical technique used for estimating independent components (ICs) by maximizing the non-Gaussianity of ICs, maximizing the likelihood of ICs, or minimizing mutual information between ICs [37]. Furthermore, EEMD was integrated with ICA (EEMD-ICA) to suppress motion artifacts from EEG in a different study [33].

In a recent study, Gajbhiye et al. [38] employed techniques grounded in multiresolution total variation and multiresolution weighted total variation to eradicate artifacts from EEG signals. Additionally, Gajbhiye et al. [39] utilized wavelet domain-optimized Savitzky–Golay filters for noise removal in EEG signals.

The existing EMD-based approaches are computationally complex and take longer to implement than the EWT algorithm [40,41]. They also have drawbacks of mode mixing, iterative runs, and its requirement of the approach to determine the extrema points and stopping criteria [42]. To solve these significant sifting stopping criteria such as standard deviation criterion [43], multi-threshold criterion, orthogonality criterion and bandwidth criterion [44] have been proposed. Albeit these criteria are not self-adaptive, we need to set the threshold to define the process which results in inconsistent performance based on the nature of the signal [42]. Similarly, even discrete wavelet transform (DWT) requires us to select the levels of decomposition manually [38]. The SSA method also requires manual selection of window length and number of components.

This paper attempts to solve these problems by using empirical wavelet transform (EWT) which is computationally more efficient than EMD and it is a self-adaptive technique [45]. The wavelets which are used to extract the intrinsic mode functions (IMFs) are tailor-made for each input signal rather than the selection of the wavelets from some prescribed dictionary. In DWT, the basis functions are fixed and do not change with the change in frequency information. EMD is an adaptive technique which adapts as per the change in frequency information. However, in EMD, there is no mathematical model and also the selection of stopping criteria is not well defined. Therefore, EWT is preferred over both the signal decomposition techniques as it is adaptive to frequency change and has a well-defined mathematical background. EWT has been extensively used for several applications such as noise suppression in speech signals, ECG signal contamination removal, denoising the vibration signals and recognizing the bearing faults, Ocular artifact removal using FBSE-EWT, Seismic noise attenuation using waveform classification [46–50].

Table 1
Comparison of denoising techniques based on the decomposition technique.

Method	Frequency adaptive	Low computational complexity
EMD-based approaches	✔	×
DWT-based approaches	×	✔
EEMD-based approaches	✔	×
EWT-based approach (our proposed approach)	✔	✔

A brief summary of the above discussion in the form of a qualitative comparison between our proposed method and other state of the art methods is presented in the Table 1. A more thorough and quantitative discussion between them is presented in Section 3.

The key highlights of the paper are as follows:

1. Developed EWT-based automated approaches for motion artifact suppression in EEG signals.
2. Explored two approaches namely, EWT-principal component analysis (PCA) based approach and IMF-variance based approach for artifact suppression.
3. IMF-variance based approach has outperformed existing approaches and found to be effective in motion artifact suppression.

2. Proposed methods

The block diagram in Figs. 1(a) and 1(b) present the proposed EWT-PCA and EWT-based denoising methods, respectively. The EEG signals are obtained from the publicly available Physionet database (detailed in Section 2.1). The Physionet database is quite robust and has only a few drawbacks such as the limited size of the dataset and the technical limitations of the EEG data acquisition system, since the entire dataset is acquired using the same equipment. The noisy EEG frames are identified using the trigger data provided with the EEG dataset. The decomposition of EEG signals are performed using EWT. For the EWT-PCA method, the first two principal components (PCs) of the IMF matrix are reconstructed to obtain the noise which is then subtracted from the artifact-contaminated EEG signal to obtain the denoised signal. For the EWT-based method, the variance of each IMF is calculated, and the two IMFs with the highest variance are set to zero. The denoised signal is then reconstructed from the remaining IMFs.

2.1. EEG database

The data used in this work was obtained from a publicly available Physionet database, specifically, the motion artifact contaminated fNIRS (functional Near Infrared Spectroscopy) EEG data [45,51]. The data consists of 23 different EEG signals recorded from the pre-frontal cortex. With a total of 2 recordings, one each from one of the 2 transducers. One transducer was disturbed to generate motion artifacts within 2-min intervals and the second one was kept undisturbed. The motion of the disturbed transducer was accurately recorded along with the lack of motion of the undisturbed second transducer by the use of the outputs of 3-axis accelerometers affixed to each transducer [45]. The accelerometer signals were digitally resampled at 2048 Hz to match the EEG signals [45].

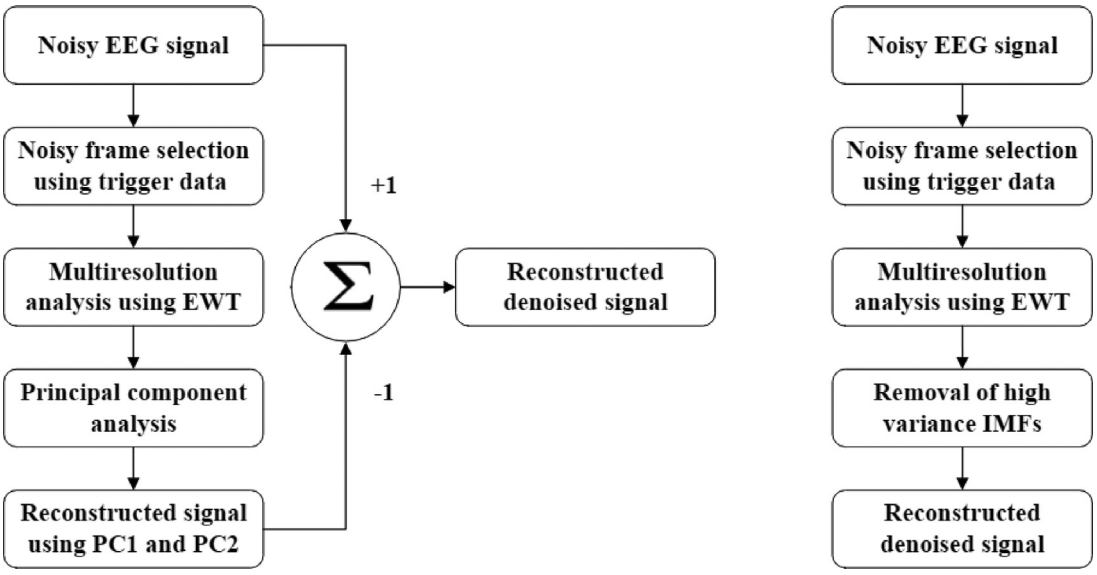

Fig. 1. Block diagram of the proposed methods: (a) EWT-PCA and (b) EWT-based denoising.

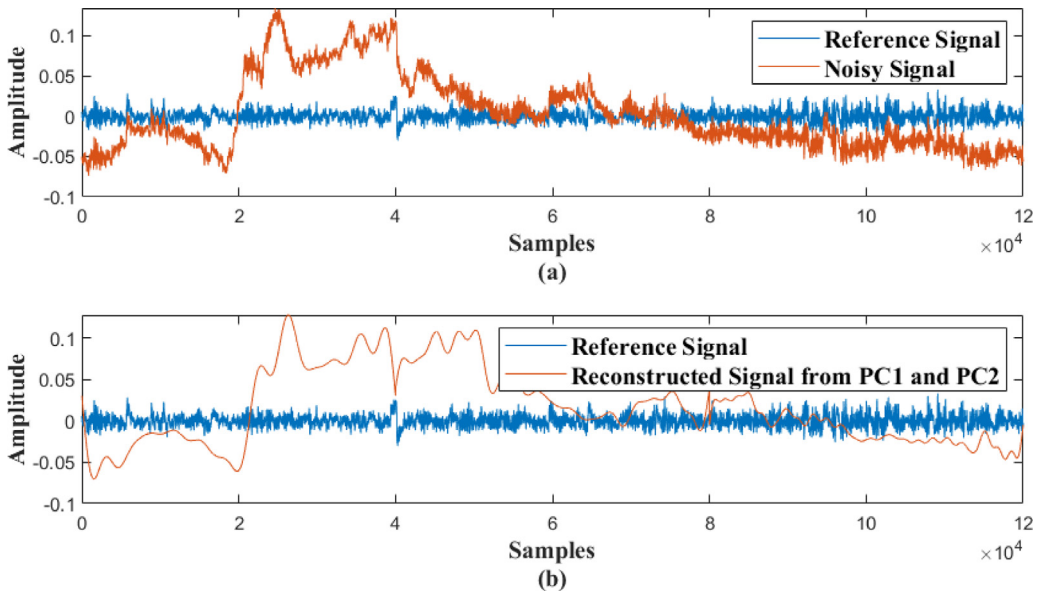

Fig. 2. (a) Superimposed noisy (red) and reference (blue) signals for EEG1. (b) The reconstructed signal from the first two principal components of the noisy EEG1 signal. (For interpretation of the references to color in this figure legend, the reader is referred to the web version of this article.)

Hence, there are two signals per EEG recording: one noisy signal containing motion artifacts and the other non-noisy reference signal. The comparison of the noisy signal with the reference signal reveals a high value of correlation coefficient in the time duration when the transducer was not manipulated, and a lower value of correlation was observed during the motion-contaminated intervals [45]. The non-motion contaminated signal is used as the reference to validate the proposed EWT-based denoising approach of the noisy signals.

The database mentions the frames of the signal containing motion artifact using trigger data which specifies the frames that contain the artifact. Using that data, we have isolated the frames containing motion artifacts. The signal was multiplied by 0.001 at all points since the database annotated that the gain of their amplifier was 1000 [45] to ensure the use of actual recordings. The noisy and reference signals for the second noisy frame of EEG1 (EEG1 represents the first EEG signal in the dataset) are shown in Fig. 2.

2.2. Method 1: EWT-based decomposition

Empirical wavelet transform (EWT) is applied to decompose the EEG signal [52]. It is an adaptive technique, typically used for analyzing non-stationary signals. Non-stationary signals have dynamically changing components *i.e.,* no fixed period. To analyze and capture the information from the non-stationary signals, adaptive techniques are found to be more suitable when compared to non-adaptive techniques [53]. Discrete wavelet transform, Fourier transform are non-adaptive techniques as they have fixed basis functions which fails to capture varying information in the non-stationary signals.

EWT analyzes a signal by extracting or decomposing the signal into different frequency components or sub-bands of a signal. Firstly, the Fourier spectrum of the signal is computed. Then, the Fourier spectrum is segmented based on the information present in the form of frequency. Further, the adaptive filter banks are formed with help of the boundaries of the segments. Finally, these sub-bands are extracted

by designing wavelet filter banks customized for input signals. The sub-band refers to a signal which has a narrow frequency range in the Fourier spectrum and is centered around a specific frequency. Different sub-bands present in the input signal represent the narrow-band information at different locations of the frequency spectrum.

The adaptability of the wavelets is obtained by considering where the information is present in the spectrum of the analyzed signal [52] and then partitioning the Fourier spectrum accordingly. The major steps involved in EWT are as follows:

Firstly, the Fourier spectrum $X(\omega)$ is computed for the noisy input signal $x(n)$. Then $X(\omega)$ is partitioned to obtain the center frequencies $\{f_1, f_2, \ldots, f_N\}$ by detecting the local maxima of the Fourier spectrum [46]. Thereafter, the boundaries are constructed by considering the neighboring center frequencies. Boundaries Ω_i can be present on the mid-points between two consecutive frequencies as:

$$\Omega_i = \left(f_i + f_{i+1}\right)/2. \tag{1}$$

After determining the boundaries, the approximation coefficients $W_x(1,t)$ and detailed coefficients $W_x(n,t)$ can be found using the scaling function ϕ_1(t) and the empirical wavelet function $\Psi_n(\omega)$, respectively [46].

$$W_x(1,t) = F^{-1}\left(X(\omega).\phi_1(\omega)\right) \tag{2}$$

$$W_x(n,t) = F^{-1}\left(X(\omega).\Psi_n(\omega)\right) \tag{3}$$

Here, F^{-1} represents the inverse Fourier transform. The decomposition of the signal $x(n)$ into its IMFs is mathematically expressed as follows:

$$x(n) = \sum_{n=1}^{N} IMF_n \tag{4}$$

where N is the number of intrinsic modes obtained from EWT. The intrinsic mode functions can be obtained by convolving the scaling function $\phi_1(t)$ with the approximation coefficients $W_x(1,t)$ and empirical wavelet functions $\Psi_n(t)$ with their corresponding detail coefficients $W_x(n,t)$ [46] as shown below:

$$IMF_1 = W_x(1,t) * \phi_1(t) \tag{5}$$

$$IMF_n = W_x(n,t) * \Psi_n(t), \forall n > 1 \tag{6}$$

2.3. Method 2: EWT-PCA-based denoising

Principal component analysis (PCA) is found to be effective in noise suppression of EEG signals [54]. Motivated by the success of PCA in noise suppression, we explore PCA along with EWT. In this work, PCA is applied to the IMFs obtained from (5–6). Each column in multiresolution analysis (MRA) represents one IMF. PCA isolates the orthogonal, uncorrelated components. The principal components (PCs) with the highest variance correspond to noise when the motion artifact has higher energy than the signal [55]. The signal reconstructed from the first two PCs of the second noisy frame of EEG 2 is shown in Fig. 2 (b).

Each IMF is standardized, and the covariance matrix (Cov) is calculated as follows:

$$IMf_i = \left(IMF_i - \mu_i\right)/\sigma_i \tag{7}$$

$$Cov(i,j) = E\left(IMf_i \cdot IMf_j^T\right) \tag{8}$$

where μ_i and σ_i are the mean and standard deviation for IMf_i. The eigenvalues and eigenvectors are calculated for the covariance matrix. The nth PC, corresponding to the eigenvector with the nth highest eigenvalue is calculated as:

$$PC_n = Eig_n^T \cdot {x_1}^T \tag{9}$$

The PCs with the highest variance are retained and the remaining are discarded. In this work, we have retained the first two PCs to get reconstructed signal $x'(n)$. The denoised signal $x_2(n)$ is obtained by subtracting $x'(n)$ from the original noisy signal.

$$x'(n) = PC1 + PC2 \tag{10}$$

$$x_2(n) = x(n) - x'(n) \tag{11}$$

2.4. IMF-variance based denoising

In general, the variance of IMFs with noise is high when compared to the variance of IMFs without noise [56]. Therefore, in this approach, the IMFs with the highest variance are set to zero to get the noise-suppressed signal.

Variance is calculated for each of the IMFs as follows:

$$Var_{imf} = \frac{\sum_{i=1}^{n}\left(IMF_i - \mu\right)^2}{n} \tag{12}$$

here n, and μ represents the length, and mean of IMf_i, respectively. The two IMFs with the highest variance are removed, and the denoised signal is reconstructed using Eq. (4).

2.5. Performance metrics

To quantify the performance of our approach, we have explored three metrics namely, average signal to noise ratio (ΔSNR), correlation coefficient (η) [28] and improvement in root mean square error (RMSE). The difference in signal-to-noise ratio (SNR) before and after applying the denoising technique is shown by ΔSNR and mathematically shown as:

$$\Delta SNR = SNR_{after} - SNR_{before} \tag{13}$$

where SNR_{before} and SNR_{after} are defined as:

$$SNR_{before} = 10 \times log\left(\frac{\|x_{ref}\|^2}{\|x_{ref} - x(n)\|^2}\right) \tag{14}$$

$$SNR_{after} = 10 \times log\left(\frac{\|x_{ref}\|^2}{\|x_{ref} - x_2(n)\|^2}\right) \tag{15}$$

where x_{ref} is the reference EEG.

The second metric, the percentage reduction in a correlation coefficient (η) is defined as follows:

$$\eta = \left[1 - \frac{1-\rho_{after}}{1-\rho_{before}}\right] \times 100 \tag{16}$$

where $\rho_{\text{before}} = \rho(x_{ref}, x(n))$ and $\rho_{\text{after}} = \rho(x_{ref}, x_2(n))$ are the correlation coefficients before and after removing the motion artifact.

The third metric is the improvement in RMSE. The RMSE before and after applying the denoising techniques are shown as follows:

$$RMSE = \frac{1}{N}\sum_{n=i}^{N}(x_{ref} - x_i)^2 \tag{17}$$

Where x_i is the noisy or denoised signal and x_{ref} is the reference signal. The improvement in RMSE is the difference between the RMSE of the noisy and denoised signal.

3. Results and discussions

We have evaluated the performance of the proposed EWT-PCA and EWT-based denoising techniques using all 23 EEGs in the database. The summary statistics of the results are provided in Table 2. The average value of ΔSNR and η along with the deviation is 26.78 ± 3.10 dB and 52.92 ± 16.38%, respectively for the EWT-PCA-based denoising technique. Similarly, 28.26 ± 4.28 dB and 55.00 ± 13.08% are the average value of ΔSNR and η, respectively for EWT-based denoising techniques.

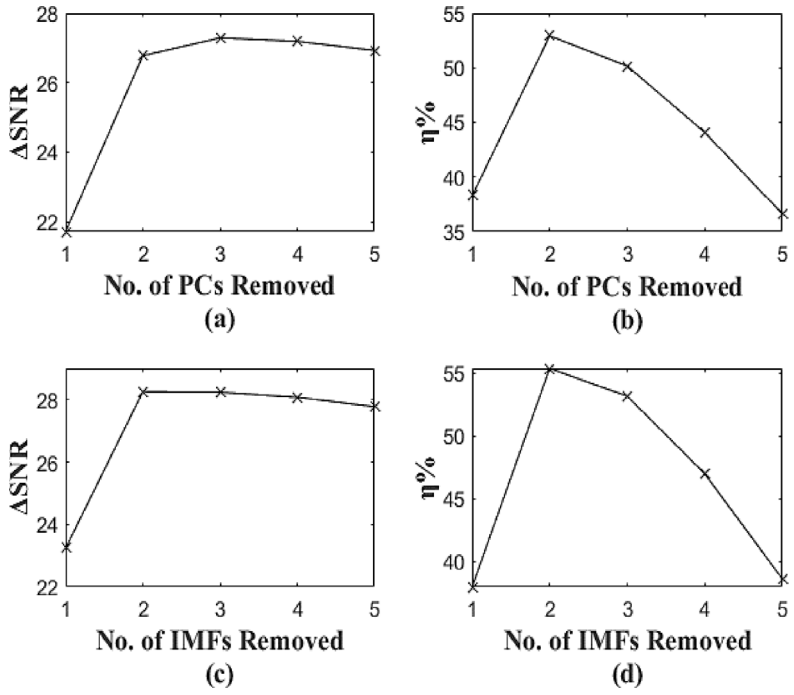

Fig. 3. (a) Variation of ΔSNR with the number of principal components retained. (b) Variation of η% with the number of principal components retained. (c) Variation of ΔSNR with the number of high-frequency IMFs removed. (b) Variation of η with the number of high-frequency IMFs removed.

Table 2
Summary statistics obtained for proposed denoising techniques using the Physionet database.

Measure	EWT-PCA based denoising			EWT based denoising		
	ΔSNR (dB)	η (%)	RMSE	ΔSNR (dB)	η (%)	RMSE
Mean	26.78	52.92	0.156	28.26	55.00	0.157
Std Dev	3.10	16.38	0.078	4.28	13.08	0.079
Minimum	21.08	20.78	–	19.92	29.09	–
Maximum	33.72	78.24	–	35.58	71.76	–

Table 3
Comparison of our method with the existing methods developed for motion artifact removal.

Method	ΔSNR (dB)	η (%)
DWT and thresholding [28]	8.08 ± 4.01	55.3 ± 35.40
EMD and IMF selection [31]	7.28 ± 3.67	43.2 ± 31.20
EEMD and IMF selection [28]	8.21 ± 3.82	52.2 ± 36.30
EMD-ICA [31]	7.47 ± 3.53	44.1 ± 30.80
EMD-CCA [31]	7.32 ± 3.67	43.4 ± 31.30
EEMD-ICA [31]	8:22 ± 3:81	52:3 ± 36:20
EEMD-CCA [31]	8:21 ± 3:82	52:2 ± 36:40
SSA [57]	11:16 ± 3:80	61:35 ± 21:68
EEMD-ICA-DWT [58]	21.80 ± 2.30	–
EEMD-ICA-SWT [58]	22.48 ± 2.00	–
EWT-PCA (proposed approach)	26.78 ± 3.10	52.92 ± 16.38
IMF-variance based (proposed approach)	28.26 ± 4.28	55.00 ± 13.08

The EWT-based denoising yielded better performance than the EWT-PCA-based EEG denoising, and also proved to be computationally more efficient.

The plot of ΔSNR and η with respect to the number of PCs is shown in Fig. 3(a-b). It can be seen that retaining more than two PCs improves the ΔSNR value but η value decreases. Therefore, due to this reason, the number of PCs is fixed to two. On the other hand, the plot of ΔSNR and η with respect to the number of high variance IMFs removed is shown in Fig. 3(c-d). It can be observed that removing 2 high-variance IMFs gave the best performance.

The motion artifact contaminated EEG signal, reference EEG signal, and denoised EEG signal are shown in Fig. 4 for EEG6 (EEG6 represents the sixth EEG signal in the dataset) for both proposed denoising methods. The motion artifacts are eliminated from the original noisy EEG signal. The ΔSNR and η% values obtained for EEG6 are 27.24 dB and 66.01%, respectively using the EWT-PCA method. But the EWT-based method obtained the value of 27.92 dB and 67.88% for ΔSNR and η, respectively.

For the proposed EWT-PCA denoising technique, the maximum value of ΔSNR obtained was 33.72 dB for EEG5 and the maximum value of η was 78.24% for EEG2. The minimum value of ΔSNR obtained was 21.08 dB for EEG12 and the minimum value of η was 20.78% for EEG15. For the EWT-based denoising technique, the maximum value of ΔSNR obtained was 33.00 dB for EEG10 and the maximum value of η was 71.76% for EEG6. The minimum value of ΔSNR obtained was 19.92 dB for EEG1 and the minimum value of η was 29.09% for EEG15.

A quantitative comparison based on performance of the proposed EWT-based denoising technique along with the state-of-the-art methods developed for motion artifact removal from EEG signals are presented in Table 3. The proposed IMF-variance-based approach has the highest ΔSNR among the approaches mentioned and has a comparable correlation coefficient percentage η with only SSA-based denoising method with higher η%. However, it can be noted that the SSA-based denoising has a higher standard deviation implying the results given by it may have a high variance. The experimental results presented in this section demonstrate the effectiveness of the proposed approaches in suppressing motion artifacts in EEG signals.

For our future endeavors, we plan to perform our experiments on a larger EEG database. Also, we would like to explore the proposed approach in other research problems such as based brain–computer interfaces [59] and meal onset detection based on sound signals [60] where artifact suppression plays is essential. In addition, we plan to explore the power of EWT and advanced deep learning approaches such as

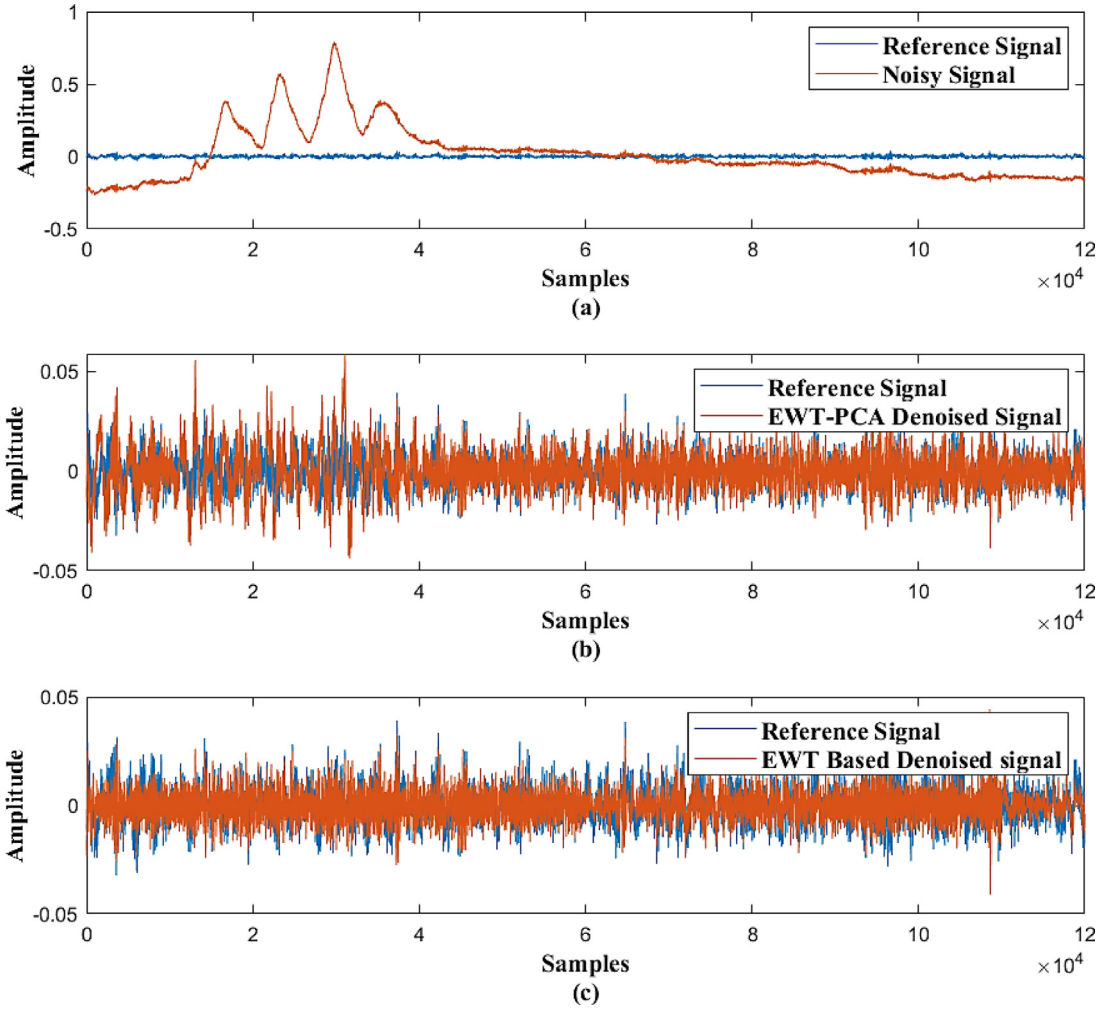

Fig. 4. (a) Superimposed reference signal and motion artifact contaminated signals for EEG6. (b) EWT-PCA denoised signal superimposed with a reference signal for EEG6. (c) EWT-based denoised signal superimposed with a reference signal for EEG6.

Multi-Stage Temporal Convolutional Network for Action Segmentation (MS-TCN) [61] for artifact suppression.

4. Conclusions

In this paper, we have proposed the EWT-based approaches for the removal of motion artifacts from EEG signals. The proposed IMF-variance-based approach achieved an average ΔSNR and η values of 28.26 dB and 55.00%, respectively. Our experimental results suggest that the proposed approach can be employed to suppress the motion artifact noise in EEG signals. Our results also suggest that the IMF-variance-based approach is more effective in noise suppression than the EWT-PCA approach and the existing approaches in the literature.

Declaration of competing interest

The authors declare the following financial interests/personal relationships which may be considered as potential competing interests: Dr. Subrata Chakraborty (Co-Guest Editor, Emerging Trends in Healthcare Decision Support Systems)

Data availability

Public dataset.

References

[1] J.C. Henry, Electroencephalography: basic principles, clinical applications, and related fields, Neurology 67 (11) (2006) 2092.
[2] M. Nuwer, Assessment of digital EEG, quantitative EEG, and EEG brain mapping: Report of the American academy of neurology and the American clinical neurophysiology society*[Retired], Neurology 49 (1) (1997) 277–292.
[3] S.K. Khare, U.R. Acharya, Adazd-net: Automated adaptive and explainable Alzheimer's disease detection system using EEG signals, Knowl.-Based Syst. 278 (2023) 110858.
[4] M. Amini, M.M. Pedram, A. Moradi, M. Ouchani, Diagnosis of Alzheimer's disease by time-dependent power spectrum descriptors and convolutional neural network using EEG signal, Comput. Math. Methods Med. 2021 (2021).
[5] S. Siuly, Y. Guo, O.F. Alcin, Y. Li, P. Wen, H. Wang, Exploring deep residual network based features for automatic schizophrenia detection from EEG, Phys. Eng. Sci. Med. 46 (2) (2023) 561–574.
[6] M. Ouchani, S. Gharibzadeh, M. Jamshidi, M. Amini, A review of methods of diagnosis and complexity analysis of Alzheimer's disease using EEG signals, BioMed Res. Int. 2021 (2021) 1–15.
[7] J.E. Goodwin, G.E. Hall, The human electroencephalogram and its clinical significance, Can. Med. Assoc. J. 41 (2) (1939) 146.
[8] M. Sharma, J. Tiwari, V. Patel, U.R. Acharya, Automated identification of sleep disorder types using triplet half-band filter and ensemble machine learning techniques with eeg signals, Electronics 10 (13) (2021) 1531.
[9] S. Finnigan, M. Walsh, S.E. Rose, J.B. Chalk, Quantitative EEG indices of sub-acute ischaemic stroke correlate with clinical outcomes, Clin. Neurophysiol. 118 (11) (2007) 2525–2532.
[10] O. Ortolani, A. Conti, A. Di Filippo, C. Adembri, E. Moraldi, A. Evangelisti, M. Maggini, S.J. Roberts, EEG signal processing in anaesthesia. Use of a neural

network technique for monitoring depth of anaesthesia, Br. J. Anaesth. 88 (5) (2002) 644–648.
[11] B. Jiao, R. Li, H. Zhou, K. Qing, H. Liu, H. Pan, Y. Lei, W. Fu, X. Wang, X. Xiao, X. Liu, Neural biomarker diagnosis and prediction to mild cognitive impairment and Alzheimer's disease using EEG technology, Alzheimer's Res. Therapy 15 (1) (2023) 1–14.
[12] B. Oltu, M.F. Akşahin, S. Kibaroğlu, A novel electroencephalography based approach for Alzheimer's disease and mild cognitive impairment detection, Biomed. Signal Process. Control 63 (2021) 102223.
[13] M. Van Mierlo Papadopoulou, E. Carrette, P. Boon, S. Vandenberghe, K. Vonck, D. Marinazzo, Functional brain connectivity from EEG in epilepsy: Seizure prediction and epileptogenic focus localization, Prog. Neurobiol. 121 (2014) 19–35.
[14] X. Liu, J. Wang, J. Shang, J. Liu, L. Dai, S. Yuan, Epileptic seizure detection based on variational mode decomposition and deep forest using EEG signals, Brain Sci. 12 (10) (2022) 1275.
[15] M.S. Nafea, Z.H. Ismail, Supervised machine learning and deep learning techniques for epileptic seizure recognition using EEG signals—A systematic literature review, Bioengineering 9 (12) (2022) 781.
[16] I. Ahmad, X. Wang, M. Zhu, C. Wang, Y. Pi, J.A. Khan, S. Khan, O.W. Samuel, S. Chen, G. Li, EEG-based epileptic seizure detection via machine/deep learning approaches: A systematic review, Comput. Intell. Neurosci. 2022 (2022).
[17] S. Gannouni, A. Aledaily, K. Belwafi, H. Aboalsamh, Emotion detection using electroencephalography signals and a zero-time windowing-based epoch estimation and relevant electrode identification, Sci. Rep. 11 (1) (2021) 7071.
[18] V.M. Joshi, R.B. Ghongade, EEG based emotion detection using fourth order spectral moment and deep learning, Biomed. Signal Process. Control 68 (2021) 102755.
[19] S. Gannouni, A. Aledaily, K. Belwafi, H. Aboalsamh, Electroencephalography based emotion detection using ensemble classification and asymmetric brain activity, J. Affect. Disord. 319 (2022) 416–427.
[20] S. Chaabene, B. Bouaziz, A. Boudaya, A. Hökelmann, A. Ammar, L. Chaari, Convolutional neural network for drowsiness detection using EEG signals, Sensors 21 (5) (2021) 1734.
[21] L. Guarda, J.E. Tapia, E.L. Droguett, M. Ramos, A novel Capsule Neural Network based model for drowsiness detection using electroencephalography signals, Expert Syst. Appl. 201 (2022) 116977.
[22] K. Polat, A.B. Aygun, A.R. Kavsaoglu, EEG based brain-computer interface control applications: A comprehensive review, J. Bionic Mem. 1 (1) (2021) 20–33.
[23] Z. Oralhan, B. Oralhan, M.M. Khayyat, S. Abdel-Khalek, R.F. Mansour, 3D input convolutional neural network for SSVEP classification in design of brain computer interface for patient user, Comput. Math. Methods Med. 2022 (2022).
[24] S. Aggarwal, N. Chugh, Review of machine learning techniques for EEG based brain computer interface, Arch. Comput. Methods Eng. (2022) 1–20.
[25] D.M. White, C.A. Van Cott, EEG artifacts in the intensive care unit setting, Am. J. Electroneurodiag. Technol. 50 (1) (2010) 8–25.
[26] A. Bertrand, V. Mihajlović, B. Grundlehner, C. Van Hoof, M. Moonen, Motion artifact reduction in EEG recordings using multi-channel contact impedance measurements, in: 2013 IEEE Biomedical Circuits and Systems Conference, BioCAS, IEEE, 2013, pp. 258–261.
[27] G. Gargiulo, R.A. Bifulco, M. Cesarelli, C. Jin, A. van Schaik, A mobile EEG system with dry electrodes, in: IEEE Biomedical Circuits and Systems Conference, IEEE, 2008, pp. 273–276.
[28] V. Mihajlovic, G.G. Molina, J. Peuscher, To what extent can dry and water-based EEG electrodes replace conductive gel ones? in: Proc. BIODEVICES Conference, Vilamoura, Algarve, Portugal, 2012.
[29] R. Vautard, P. Yiou, M. Ghil, Singular-spectrum analysis: A toolkit for short, noisy chaotic signals, Physica D 58 (1–4) (1992) 95–126.
[30] A.K. Maddirala, R.A. Shaik, Motion artifact removal from single channel electroencephalogram signals using singular spectrum analysis, Biomed. Signal Process. Control 30 (2016) 79–85.
[31] K.T. Sweeney, S.F. McLoone, T.E. Ward, The use of ensemble empirical mode decomposition with canonical correlation analysis as a novel artifact removal technique, IEEE Trans. Biomed. Eng. 60 (1) (2012) 97–105.
[32] N.E. Huang, Z. Shen, S.R. Long, M.C. Wu, H.H. Shih, Q. Zheng, N.C. Yen, C.C. Tung, H.H. Liu, The empirical mode decomposition and the Hilbert spectrum for nonlinear and non-stationary time series analysis, Proc. R. Soc. Lond. Ser. A Math. Phys. Eng. Sci. 454 (1971) (1998) 903–995.
[33] Z. Wu, N.E. Huang, Ensemble empirical mode decomposition: a noise-assisted data analysis method, Adv. Adapt. Data Anal. 1 (01) (2009) 1–41.
[34] A.N. Akansu, R.A. Haddad, Multiresolution Signal Decomposition: Transforms, Subbands, and Wavelets, Academic Press, 2001.
[35] M. Hosseinzadeh, Robust control applications in biomedical engineering: Control of depth of hypnosis, in: Control Applications for Biomedical Engineering Systems, Academic Press, 2020, pp. 89–125.
[36] S. Mahmud, M.S. Hossain, M.E. Chowdhury, M.B.I. Reaz, MLMRS-Net: Electroencephalography (EEG) motion artifacts removal using a multi-layer multi-resolution spatially pooled 1D signal reconstruction network, Neural Comput. Appl. 35 (11) (2023) 8371–8388.
[37] A. Tharwat, Independent component analysis: An introduction, Appl. Comput. Inform. 17 (2) (2021) 222–249.
[38] P. Gajbhiye, R.K. Tripathy, A. Bhattacharyya, R.B. Pachori, Novel approaches for the removal of motion artifact from EEG recordings, IEEE Sens. J. 19 (22) (2019) 10600–10608.
[39] P. Gajbhiye, N. Mingchinda, W. Chen, S.C. Mukhopadhyay, T. Wilaiprasitporn, R.K. Tripathy, Wavelet domain optimized Savitzky–Golay filter for the removal of motion artifacts from EEG recordings, IEEE Trans. Instrum. Meas. 70 (2020) 1–11.
[40] O. Singh, R.K. Sunkaria, Powerline interference reduction in ECG signals using empirical wavelet transform and adaptive filtering, J. Med. Eng. Technol. 39 (1) (2015) 60–68.
[41] V.S. Geetikaverma, Empirical wavelet transform & its comparison with empirical mode decomposition: a review, Int. J. Appl. Eng. 4 (5) (2016).
[42] R. Ranjan, B.C. Sahana, A.K. Bhandari, Motion artifacts suppression from EEG signals using an adaptive signal denoising method, IEEE Trans. Instrum. Meas. 71 (2022) 1–10.
[43] A.O. Boudraa, J.C. Cexus, EMD-based signal filtering, IEEE transactions on instrumentation and measurement 56 (6) (2007) 2196–2202.
[44] X.D. Niu, L.R. Lu, J. Wang, X.C. Han, X. Li, L.M. Wang, An improved empirical mode decomposition based on local integral mean and its application in signal processing, Math. Probl. Eng. 2021 (2021) 1–30.
[45] K.T. Sweeney, H. Ayaz, T.E. Ward, M. Izzetoglu, S.F. McLoone, B. Onaral, A methodology for validating artifact removal techniques for physiological signals, IEEE Trans. Inform. Technol. Biomed. 16 (5) (2012) 918–926.
[46] T.S. Kumar, M.A. Hussain, V. Kanhangad, Classification of voiced and non-voiced speech signals using empirical wavelet transform and multi-level local patterns, in: 2015 IEEE International Conference on Digital Signal Processing, DSP, IEEE, 2015, pp. 163–167.
[47] P. Gajbhiye, R.K. Tripathy, R.B. Pachori, Elimination of ocular artifacts from single channel EEG signals using FBSE-EWT based rhythms, IEEE Sens. J. 20 (7) (2019) 3687–3696.
[48] X. Xu, Y. Liang, P. He, J. Yang, Adaptive motion artifact reduction based on empirical wavelet transform and wavelet thresholding for the non-contact ECG monitoring systems, Sensors 19 (13) (2019) 2916.
[49] S.N. Chegini, A. Bagheri, F. Najafi, Application of a new EWT-based denoising technique in bearing fault diagnosis, Measurement 144 (2019) 275–297.
[50] W. Chen, M. Bai, H. Song, Seismic noise attenuation based on waveform classification, J. Appl. Geophys. 167 (2019) 118–127.
[51] A.L. Goldberger, L.A. Amaral, L. Glass, J.M. Hausdorff, C. Ivanov, R.G. Mark, J.E. Mietus, G.B. Moody, C.K. Peng, H.E. Stanley, PhysioBank, PhysioToolkit, and PhysioNet: components of a new research resource for complex physiologic signals, circulation 101 (23) (2000) e215–e220.
[52] J. Gilles, Empirical wavelet transform, IEEE Trans. Signal Process. 61 (16) (2013) 3999–4010.
[53] S. Maheshwari, R.B. Pachori, U.R. Acharya, Automated diagnosis of glaucoma using empirical wavelet transform and correntropy features extracted from fundus images, IEEE J. Biomed. Health Inf. 21 (3) (2017) 803–813.
[54] X. Yu, M.Z. Aziz, M.T. Sadiq, Z. Fan, G. Xiao, A new framework for automatic detection of motor and mental imagery EEG signals for robust BCI systems, IEEE Trans. Instrum. Meas. 70 (2021) 1–12.
[55] I. Romero, PCA-based noise reduction in ambulatory ECGs, in: 2010 Computing in Cardiology, IEEE, 2010, pp. 677–680.
[56] Y.X. Li, L. Wang, A novel noise reduction technique for underwater acoustic signals based on complete ensemble empirical mode decomposition with adaptive noise, minimum mean square variance criterion and least mean square adaptive filter, Def. Technol. 16 (3) (2020) 543–554.
[57] A.K. Maddirala, R.A. Shaik, Motion artifact removal from single channel electroencephalogram signals using singular spectrum analysis, Biomed. Signal Process. Control 30 (2016) 79–85.
[58] V. Roy, S. Shukla, Designing efficient blind source separation methods for EEG motion artifact removal based on statistical evaluation, Wirel. Pers. Commun. 108 (2019) 1311–1327.
[59] H. Wu, Y. Niu, F. Li, Y. Li, B. Fu, G. Shi, M. Dong, A parallel multiscale filter bank convolutional neural networks for motor imagery EEG classification, Front. Neurosci. 13 (1275) (2019).
[60] T.S. Kumar, E. Søiland, Stavdahl Ø, A.L. Fougner, Pilot study of early meal onset detection from abdominal sounds, in: 2019 IEEE E-Health and Bioengineering Conference, EHB, 2019, pp. 1–4.
[61] Y.A. Farha, J. Gall, MS-TCN: Multi-stage temporal convolutional network for action segmentation, in: Proceedings of the IEEE/CVF Conference on Computer Vision and Pattern Recognition, 2019, pp. 3575–3584.